General Disclaimer

One or more of the Following Statements may affect this Document

- This document has been reproduced from the best copy furnished by the organizational source. It is being released in the interest of making available as much information as possible.

- This document may contain data, which exceeds the sheet parameters. It was furnished in this condition by the organizational source and is the best copy available.

- This document may contain tone-on-tone or color graphs, charts and/or pictures, which have been reproduced in black and white.

- This document is paginated as submitted by the original source.

- Portions of this document are not fully legible due to the historical nature of some of the material. However, it is the best reproduction available from the original submission.

LUMIN

FINAL REPORT

on

Contract NAS8-31746

A THEORETICAL ANALYSIS OF THE MSFC HOLOGRAPHIC CORRELATION SYSTEM

by

Hua-Kuang Liu

Prepared for

National Aeronautics and Space Administration
George C. Marshall Space Flight Center
Marshall Space Flight Center, Alabama 35812

May 31, 1977

LUMIN Report No. 122-77

Lumin, Inc.
P.O. BOX 5620 TUSCALOOSA, ALABAMA 35401

A THEORETICAL ANALYSIS OF THE MSFC HOLOGRAPHIC CORRELATION SYSTEM

TABLE OF CONTENTS

Abstract

Page No.

I. Introduction 1

II. Statement of the problem and basic assumptions..... 2

III. Theoretical Analysis..... 5

IV. Conclusions..... 13

Appendix A..... 15

References..... 18

A THEORETICAL ANALYSIS OF THE MSFC HOLOGRAPHIC CORRELATION SYSTEM

Abstract

A theoretical analysis has been completed for the correlation output signal for the MSFC holographic correlation filtering system. Under appropriate assumptions, the correlation output was derived as a function of the roughness of the tested surface, the displacement of the illuminated area of the test surface, the characteristics of the optical components used in the system, and the system configuration. In addition, an approximate relationship between the displacement of the detected signal (which is focused on the photomultiplier tube) and the displacement of the illuminated area on the test surface was also derived.

A THEORETICAL ANALYSIS OF THE MSFC HOLOGRAPHIC CORRELATION SYSTEM

I. Introduction

Holographic non-destructive testing (HNDT) has a broad range of applications in the military and industrial testing of ultra-expensive and zero-defect-demanded instruments and equipment such as the main shuttle engine of NASA's space shuttles.

Most of the work of HNDT has been done in holographic interferometry, which basically involves recording and interpreting fringes resulting from the interaction between two mutually coherent wavefronts. Recently, a practical method of interpreting the interference fringes has been devised and experimentally verified.[1,2] The method enables one to determine anomalous displacement on the surface of an object semi-quantitatively. On the other hand, the technique of holographic correlation can be used to zero-in on a specific abnormal region, which can be determined by the previous holographic interferometry method. The correlation technique will give an overall number which signifies the similarity of the two wavefronts being processed. From this number, the knowledge of the stress and strain on that specific region can be found.

The correlation technique utilized a Vander Lugt filter as a matched filter in the study of the autocorrelation properties of the stressed and unstressed object.[3-8] The main reason which motivated the contracted study described in this report is due to the experimental discovery a secondary peak in the putput of the correlation intensity in the MSFC corelation system. In addition, it was found that there was no variations in the correlation signal strength when an aperture was inserted in the object beam. The anomalism of the secondary peak

was removed in the experiment after the contractor suggested that the system configuration be changed to the present one with an oblique incident object beam from its previous normal incident setup. Moreover, an object beam focusing lens was added to focus the beam on the rough test surface. The focused beam causes the scattered light from the surface to have a broader speckle pattern. A hologram made in the present system was able to produce a correlation function with a much stronger signal-to-noise ratio (about two orders of magnitude stronger than the signal-to-noise ratio obtained in the previous system). Results showed that no more secondary peak was observed. Hence the secondary peak observed before probably was due to the interference of noise to an extremely weak correlation signal. The effect of aperture, however, should be easily visualized after the theoretical analysis is presented in the following.

Section II will be the statement of the problem and the basic assumptions being made. The theoretical analysis will be provided in Section III. Section IV are the conclusions.

II. Statement of the problem and basic assumptions

A. State of the problem

A theoretical analysis is required to describe the correlation signal, detected in the holographic correlation filtering system as shown in Figure 1, as a function of the roughness of the test surface, the displacement of the illuminated area, the characteristics of the optical components, and the configuration of the system.

B. Basic assumptions

It is assumed that (1) The test surface is uniformly and isotropically rough in two dimensions with normally distributed roughness

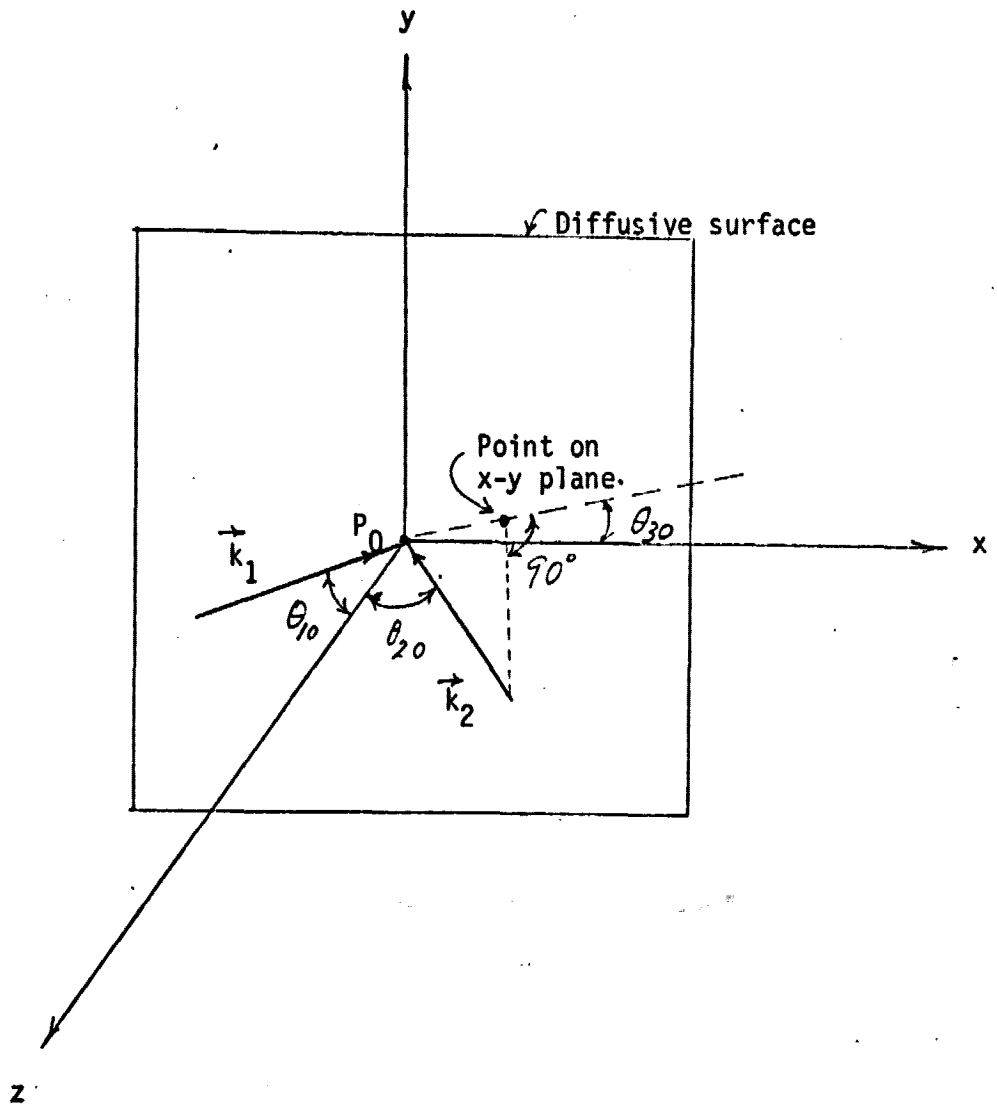

Figure 1. A diagram showing the wave vectors of the incident and reflected beams and the diffusive surface.

ζ (x,y) of zero mean ("flat"), variance σ^2, and correlation distance X. (2) Both σ and X are of similar magnitude as the optical wavelength λ or larger. (3) The radius of the laser beam, r_0, focused on the object surface is large compared with the correlation distance X and the wavelength λ.

III. Theoretical Analysis

When the laser beam strikes a point P at the surface of the object, light will be scattered. As shown in Fig. 1, the scattering angles θ_1, θ_2 and θ_3 at P may be defined according to the Bechmann's convention.[9]

θ_1 is the angle of incidence of the beam with wave vector $\vec{k}_1$ on the mean surface,

$$\theta_1 = \cos^{-1} [- (\vec{n} \cdot \vec{k}_1) / |\vec{k}_1|], \tag{1}$$

where $|\vec{k}_1| = 2\pi/\lambda$ which is the absolute value of $\vec{k}_1$ and $\vec{n}$ is the unit vector of the outer normal through the point P of the mean surface. Similarly,

$$\theta_2 = \cos^{-1} [(\vec{n} \cdot \vec{k}_2) / |\vec{k}_2|], \tag{2}$$

where $\vec{k}_2$ is the wave vector of the scattered field.

θ_3 is the angle between the planes formed by $\vec{n}$, $\vec{k}_1$ and $\vec{n}$, $\vec{k}_2$, hence

$$\theta_3 = \cos^{-1} [(\vec{n} \times \vec{k}_1) \cdot (\vec{n} \times \vec{k}_2) / (\sin\theta_1 \sin\theta_2)], \tag{3}$$

where $\theta_1 \neq 0$ and $\theta_2 \neq 0$.

If P is at the origin, these angles are defined by θ_{10}, θ_{20}, and θ_{30} respectively.

In addition, a scattering vector can be defined by

$$\vec{v} = \vec{k}_1 - \vec{k}_2 = \frac{2\pi}{\lambda} [(\sin\theta_{10} - \sin\theta_{20} \cos\theta_{30}) \vec{x} - (\sin\theta_{20} \sin\theta_{30}) \vec{y} - (\cos\theta_{10} + \cos\theta_{20}) \vec{z}], \tag{4}$$

where $\vec{x}$, $\vec{y}$, $\vec{z}$ are unit vectors in the x, y, z directions, respectively.

On the rough surface, the true local scattering angles are in general different from θ_1, θ_2, θ_3. Let $\vec{s}$ be the true local normal unit vector which can be expressed by the slopes $\zeta_x = \partial\zeta/\partial x$ and $\zeta_y = \partial\zeta/\partial y$ of the roughness $\zeta(x,y)$:

$$\vec{s} = (-\zeta_x \vec{x} - \zeta_y \vec{y} + \vec{z}) (1 + \zeta_x^2 + \zeta_y^2)^{-\frac{1}{2}} \tag{5}$$

The local scattering angles can be defined by replacing $\vec{n}$ by $\vec{s}$ in Equations (1) through (3).

Following Bechman[1], the scattered field at the far distance R_o from the surface after adaption to a Gaussian beam can be written as

$$A_2 = \frac{\frac{2\pi i}{\lambda} \exp\left[\frac{2\pi R_{oi}}{\lambda}\right] \cos\theta_{10}}{2\pi^2 r_o^2 R_o} \int_{-\infty}^{\infty}\int_{-\infty}^{\infty} P(x,y)\, F(\zeta_x, \zeta_y) \cdot e^{i \vec{v} \cdot \vec{r}}\, dx\, dy, \tag{6}$$

where $P(x,y) = \exp\left[- (x^2 \cos\theta_{10} + y^2) / r_o^2 \right]$, (7)

and $F(\zeta_x, \zeta_y)$ is defined in terms of the reflection coefficient R and the scattering angles θ_1, θ_2, and θ_3 :

$$\begin{aligned} F(\zeta_x, \zeta_y) = {} & \left[(1 - R) \sin\theta_1 + (1 + R) \sin\theta_2 \cos\alpha_3 \right] \zeta_x \\ & + \left[(1 + R) \sin\theta_2 \sin\theta_3 \right] \zeta_y \\ & - (1 + R) \cos\theta_2 + (1 - R) \cos\theta_1 . \end{aligned} \tag{8}$$

Since on the rough surface, the true local polarization state of the incident field is in general unknown, $F(\zeta_x, \zeta_y)$ can only be treated as a random variable and statistical analysis will be required.

The optical phase $\vec{v} \cdot \vec{r}$ in Eq. (6) can be written as

$$\begin{aligned} \vec{v} \cdot \vec{r} &= v_x x + v_y y + v_z (z + \zeta) \\ &= \phi(x,y) + v_z (z + \zeta), \end{aligned} \tag{9}$$

where $\phi(x,y) = v_x x + v_y y$. (10)

If a hologram is made in the configuration as shown in Fig. [2] and replaced to its original position, the hologram serves as a matched filter to the object beam when the reference beam is turned off. If the correlation lens is not in the system, the effect of the amplitude transmitted by the hologram at a distance R_o from P_o is proportional to the following correlation function with the symbol < > denoting a statistical ensemble average.

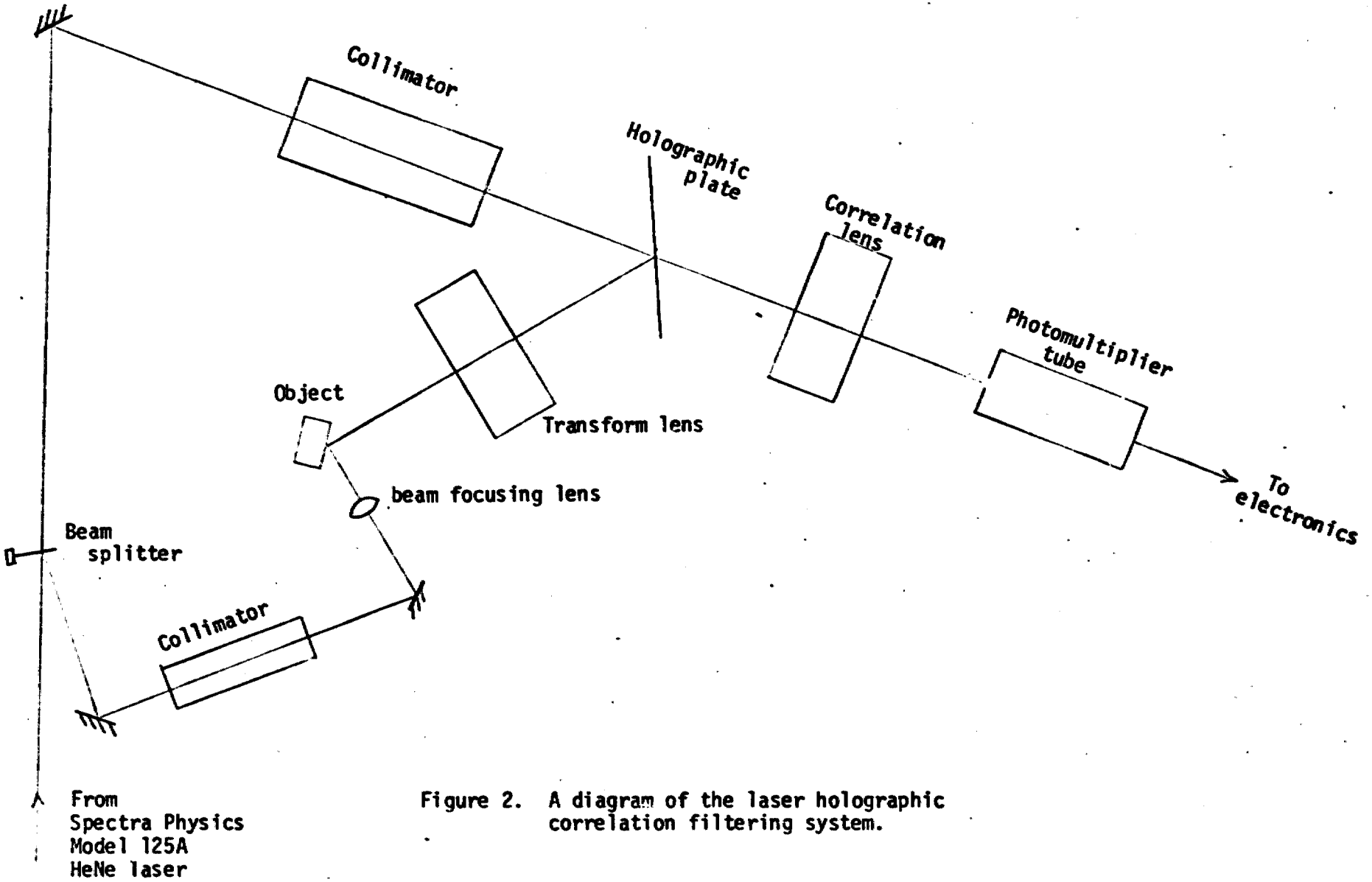

Figure 2. A diagram of the laser holographic correlation filtering system.

$$G_1 (\Delta\vec{v}) = \langle A_2 (\vec{v})\, A_2^* (\vec{v} + \Delta\vec{v}) \rangle , \tag{11}$$

Substituting Eqs. (6) and (9) into Eq. (11), one obtains

$$G_1 \frac{k^2 \cos^2 \alpha_{10}}{4\pi^4 r_0^4 R_0^2} \exp [\, i (v_{z1} z_1 - v_{z2} z_2) \,] \int_{-\infty}^{\infty}\int\int\int\int P (x_1, y_1)$$
$$P (x_2, y_2) \exp \{ i [\, \phi (x_1, y_1) - \phi (x_2, y_2) \,] \}$$
$$X \langle F (\zeta_{x1}, \zeta_{y1})\, F (\zeta_{x2}, \zeta_{y2}) \exp [\, i (v_{z1} \zeta_1 - v_{z2} \zeta_2) \,] \rangle$$
$$dx_1\, dy_1\, dx_2\, dy_2 . \tag{12}$$

In Eq. (12), ζ_2, ζ_{x2} and ζ_{y2} have to be evaluated at $x_2 - D_x$, $y_2 - D_y$, if ζ_1, ζ_{x1}, and ζ_{y1} are taken at x_1, y_1. To calculate the ensemble average as an expectation value, the joint probability density function of the six normal random variables ζ_1, ζ_2, ζ_{x1}, ζ_{x2}, ζ_{y1}, ζ_{y2} is required. Because ζ, ζ_x, and ζ_y are statistically independent, the density factorizes into three joint densities for the variable pairs (ζ_1, ζ_2), (ζ_{x1}, ζ_{x2}), (ζ_{y1}, ζ_{y2}). Each density is determined by the second moments of the variables.[10]

If the second moment of the roughness is given by

$$\langle \zeta_1 \zeta_2 \rangle = \sigma^2 C (x_1, y_1, x_2 - D_x, y_2 - D_y) , \tag{13}$$

with C the autocorrelation coefficient of the roughness.

Through some mathematical manipulation[11] one can write (See Appendix A),

$$G_1 (\Delta\vec{v}, \vec{D}) = \Omega^2 \exp [\, - (\sigma\, \Delta\, v_z)^2 / 2 \,]$$
$$\times \int_{-\infty}^{\infty}\int\int\int P (x_1, y_1)\, P (x_2, y_2)$$
$$\times \exp \{ - q^2 [\, (x_1 - x_2 + D_x)^2 + (y_1 - y_2 + D_y)^2 \,]$$
$$+ i [\, \phi (x_1, y_1) - \phi (x_2, y_2) \,] \}\, d_{x1}\, d_{y1}\, d_{x2}\, d_{y2}. \tag{14}$$

Where in the above equation,

$$\Omega = k \cos\theta_{10} \left(\langle F^2 \rangle \right)^{1/2}$$
$$/ \left(2 \pi^2 r_0^2 R_0 \right), \tag{15}$$

$$< F_1, F_2 > = < F(\zeta_{x1}, \zeta_{y1})\, F(\zeta_{x2}, \zeta_{y2}) >$$

$$= < F^2 >$$

$$= 4 < R^2 > (1 + \cos\theta_{10} \cos\theta_{20} - \sin\theta_{10} \sin\alpha_{20} \cos\theta_{30})^2 / (\cos\theta_{10} + \cos\theta_{20})^2 , \quad (16)$$

and $< R^2 >$ is the mean square of the reflection coefficient.

After the integration in Eq. (14) has been carried out, the result is a product of many exponential factors. Among these factors, only those terms that can noticeably deviate from unity are considered as significant and retained. Consequently,

$$G_1(\Delta \vec{v}, \vec{D}) = [\pi^2 r_0^2 \Omega^2 / (T S h_1 h_2 \cos\theta_{10})] \exp[-i(\bar{v}_x D_x + \bar{v}_y D_y)] \quad (17)$$

with

$$S = \exp\{-[\bar{v}_x^2 / 2h_1^2 + \bar{v}_y^2 / 2h_2^2 + 1/8\, r_0^2 (\Delta v_x^2 / \cos^2\theta_{10} + \Delta v_y^2) + 1/2 (\sigma \Delta v_z)^2]\} , \quad (18)$$

$$T = \exp[(-D_x^2 \cos^2\theta_{10} - D_y^2) / (2 r_0^2)] , \quad (19)$$

$$h_1^2 = 2q^2 + \cos^2\theta_{10} / r_0^2 , \quad (20)$$

$$h_2^2 = 2q^2 + 1 / r_0^2 , \quad (21)$$

and $\bar{v}_x = \frac{1}{2}(v_{x1} + v_{x2})$, $\Delta v_x = v_{x2} - v_{x1}$, etc. The term q^2 is described in Appendix A.

Furthermore, the correlation function for the intensity may be written as

$$G_2(\Delta \vec{v}, \vec{D}) = [\pi^2 r_0^2 \Omega^2 / (h_1 h_2 \cos\theta_{10})] [S^2(0) + S^2(\Delta \vec{v}) T^2] , \quad (22)$$

where

$$S(0) = \exp[-\bar{v}_x^2 / (2h_1^2) - \bar{v}_y^2 / (2h_2^2)] . \quad (23)$$

For a special case where $\Delta \vec{v} = 0$, Eq. (22) becomes

$$G_2(0, \vec{D}) = [\pi^2 r_0^2 \Omega^2 / (h_1 h_2 \cos\theta_{10})] S^2(0) [1 + T^2]$$
$$= K^2 \{ 1 + \exp [\frac{-1}{2r_0^2} (D_x^2 \cos^2\theta_{10} + D_y^2)] \} \quad (24)$$

with

$$K^2 = [\pi^2 r_0^2 \Omega^2 / (h_1 h_2 \cos\theta_{10})] S^2(0). \quad (25)$$

From Eq. (24), it can be seen that $G_2(0,\vec{D})$ is a function of the angles of the incident beam and the reflected beam, the radius of the beam on the rough surface, the roughness of the surface, and the displacements D_x, and D_y. When D_z varies, the radius of the beam r_0 will vary accordingly. Hence the variation of D_z will affect the magnitude of the correlation function as well.,

After the correlation lens is inserted, the scattered light from the hologram is focused at the detector surface inside the photo-multiplier tube. The Fourier transformation performed by the correlation lens undoes the Fourier transformation by the transform lens to the signal, therefore, Equations (17) and (24) can be used to describe the correlation intensity output.

When the object is translated from its original position as shown by the dotted line of Figure 3, another phenomenon will occur. The focal point at the photo-multiplier tube will also change its position due to the refraction of the laser light by the lenses and the diffraction of the beam by the hologram and the lenses. The original path of the laser beam and the path of the light after the displacement is shown by the solid and dashed lines respectively. For example, if the object is translated along the incident laser beam by an amount Δd, and the corresponding displacement of the focal point at the photo-multiplier tube is represented by $\Delta \ell$, the relationship between Δd and

$\Delta\ell$ will depend on the focal lengths of the lenses, the diffraction property of the hologram, and the geometry of the system. If a linear relationship can be assumed and if the angle between the bisector of the transform lens (the broken line in Figure 3) and the front surface of the object is θ , then the relationship between $\Delta\ell$ and Δd can be written as

$$\Delta\ell = \Delta d\left(\frac{2f_C + f_T}{f_T}\right) \cos(\theta - \theta_{10}) \ , \qquad (26)$$

where f_C and f_T are the focal length of the correlation lens and the transform lens respectively

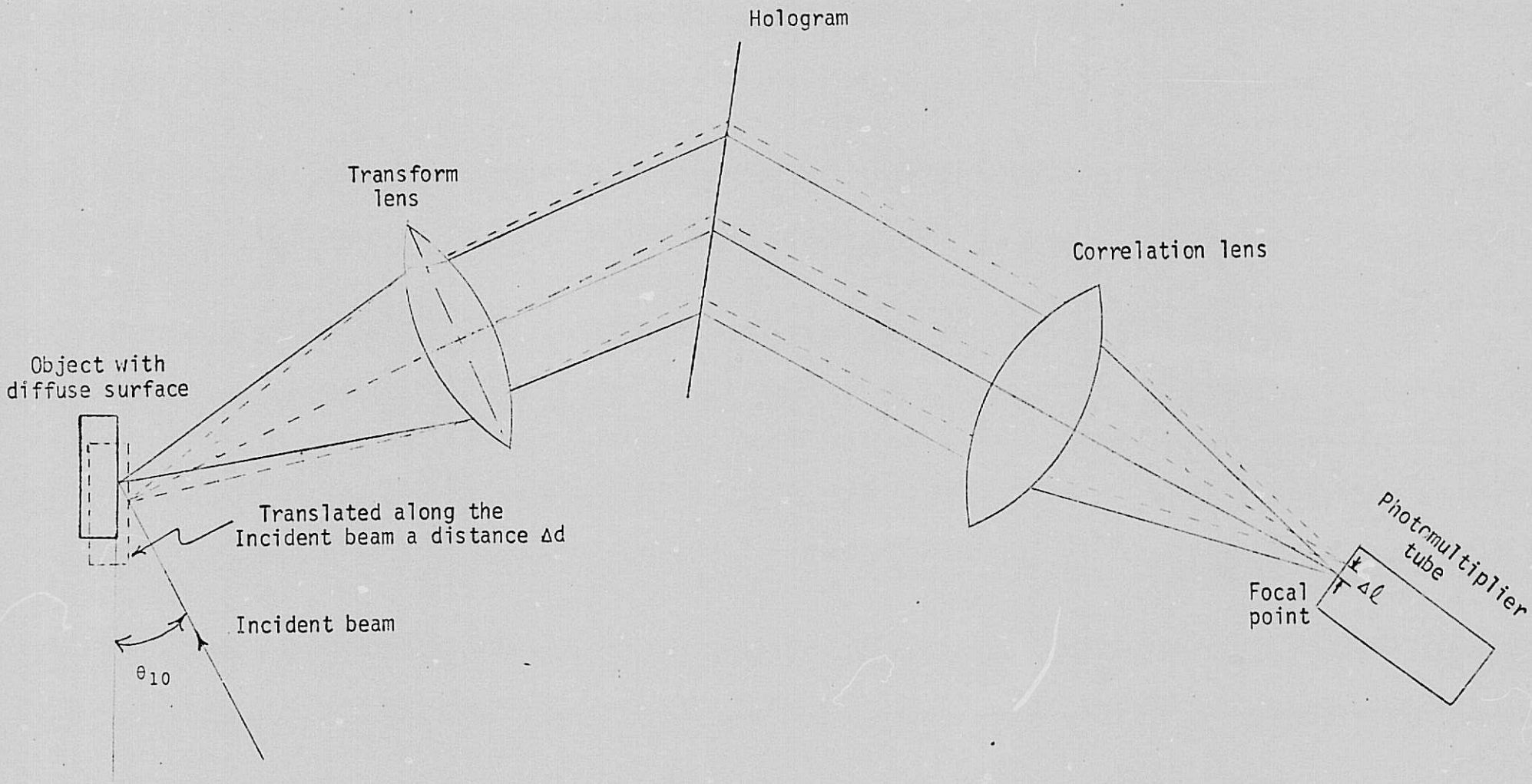

Figure 3. The displacement of the focal point on the photomultiplier tube caused by the displacement of the object (dotted line).

IV. Conclusions

A theoretical analysis has been presented for the correlation output signal for the MSFC holographic correlation filtering system. It was found that under appropriate assumptions, the correlation output may be written as a function of the roughness of the test surface, the displacement of the illuminated area of the test surface, the characteristics of the optical components involved in the system, and the system configuration.

Although no detailed comparison between the experimental result and the theoretical prediction has been made at the conclusion of this study, a few observations can be made. First, the theoretical result predicts that the correlation function has a Gaussian-form variation for the in-plane displacement and hence no secondary peak should appear. The present experimental result found no secondary peak whatsoever. Second, the holographic filter served in a statistical averaging manner, and hence its exact replacement should have no significant influence on the output signal, this agreed with the preliminary experimental results as well. Third, if an aperture of a size smaller than the object beam crosssection is inserted in the object beam of the system, it can be visualized from the theoretical analysis that its effect is to reduce the intensity of the output signal, since the total amount of light diffracted by the hologram is correspondingly reduced by the aperture.

Finally, if the variations of the parameters in the system are not sufficient to cause a variation of the output, an approximate relationship between the displacement of the detected signal (a focused spot) and that of the illuminated spot on the test surface was also derived.

Experimental verification of the predicted linear relationship should be made in future studies on this system.

APPENDIX A

Deriation of Equation (14)

If the second moment of the roughness is given by

$$\langle \zeta_1 \zeta_2 \rangle = \sigma^2 C (x_1, y_1, x_2 - D_x, y_2 - D_y), \tag{A1}$$

C being the autocorrelation coefficient of the roughness, we can apply the lemma

$$\langle H'(f)H'(f+g)\rangle = -d^2\langle H(f)H(f+g)\rangle/dg^2 , \tag{A2}$$

and obtain

$$\langle \zeta_{x1} \zeta_{x2} \rangle = -\sigma^2 \frac{\theta^2 C}{\theta \Delta_x^2}, \quad \Delta_x = x_2 - x_1 - D_x \tag{A3}$$

and

$$\langle \zeta_{y1} \zeta_{y2} \rangle = -\sigma^2 \frac{\theta^2 C}{\theta \Delta_y^2}, \quad \Delta_y = y_2 - y_1 - D_y \tag{A4}$$

Separating the ζ-dependent part of the term in angular brackets in Eq. (12), we then find by standard calculation the characteristic function

$$\begin{aligned} X(v_{z1}, -v_{z2}) &= \langle \exp[i(v_{z1}\zeta_1 - v_{z2}\zeta_2)]\rangle \\ &= \exp(-\sigma^2 \Delta v_z/2) e^{-z(1-c)}, \end{aligned} \tag{A5}$$

where we have written $\Delta v_z = v_{z2} - v_{z1}$ and

$$g = \sigma^2 v_{z1} v_{z2} . \tag{A6}$$

For ordinary rough surfaces the rms roughness σ is of the order of the wavelength λ or larger, and there holds $g >> 1$ (in fact, $g \geq 100$). Substantial contributions to the integral Eq. (12) can then come only from those aperture elements for which $C \approx 1$. We assume that C has the form

$$C = \exp[-(\Delta_x^2 + \Delta_y^2)/X^2] , \tag{A7}$$

where X is the correlation distance of the roughness, Δ_x and Δ_y have been

given in Eqs. (A3) and (A4). The function

$$p = e^{-z(1-C)}, \tag{A8}$$

with C given by Eq. (A7) can be expanded about the saddle point coordinates[13] $\Delta_x = \Delta_y = 0$ or

$$\xi_s = \mathcal{D}_x \quad \eta_s = \mathcal{D}_y \tag{A9}$$

in the plane formed by

$$\xi = x_2 - x_1, \; \eta = y_2 - y_1 \; . \tag{A10}$$

With

$$q^2 = g/X^2 \tag{A11}$$

one obtains for the first two terms

$$p = 1 - q^2 \, (\Delta_x^2 + \Delta_y^2) + \cdots , \tag{A12}$$

which will be approximated by[13]

$$p = \exp[-q^2(\Delta_x^2 + \Delta_y^2)] \; . \tag{A13}$$

For very large values of g this approximation is always very good.

For $\mathcal{D} >> r_0$ the surface elements for which $C \approx 1$, are outside the illuminated area, and contributions to G_1 do not arise because of the pupil function P(x,y), Eq. (7).

To calculate the average

$$\langle F_1 F_2 \rangle = \langle F(\zeta_{x1}, \zeta_{y1}) F(\zeta_{x2}, \zeta_{y2}) \rangle$$

in Eq. (12), we follow an approach already applied by Hagfors to the backscatter case. In essence, we assume that most of the surface slopes of importance with a particular scattering vector have values close to the mean values $\bar{\zeta}_x$ and $\bar{\zeta}_y$ defined $\bar{\zeta}_x = -v_x/v_z$ and $\bar{\zeta}_y = -v_y/v_z$. This means that $F_1 F_2$ has a maximum for $\zeta_{x1} = \zeta_{x2} = \bar{\zeta}_x$, $\zeta_{y1} = \zeta_{y2} = \bar{\zeta}_y$.

Expanding F_1F_2 about $\bar{\zeta}_x$ and $\bar{\zeta}_y$ and substituting $C \simeq 1$ in the second moments, Eqs. (A3) and (A4), we find that all terms but the zero-order term $[F(\bar{\zeta}_x, \bar{\zeta}_y)]^2$ are very small and can be neglected. In the calculation of the average we can replace θ_1, θ_2, θ_3 by the center values θ_{10}, θ_{20}, θ_{30}, respectively. We find

$$\langle F_1F_2\rangle \simeq \langle F^2\rangle = 4\langle R^2\rangle(1 + \cos\theta_{10}\cos\theta_{20} - \sin\theta_{10}\sin\theta_{20}\cos\theta_{30})^2/(\cos\theta_{10} + \cos\theta_{20})^2 . \tag{A14}$$

Here R^2 is the mean square of the reflection coefficient. For the backscatter case ($\theta_{20} = -\theta_{10}$, $\theta_{30} = 0$) one obtains the $\cos^{-2}\theta_{10}$ dependence found by Hagfors.[14]

Substituting Eqs. (A3)-(A5), (A8), (A13), and (A14) into Eq. (12) and setting

$$\Omega = k\cos\theta_{10}(\langle F^2\rangle)^{1/2}/(2\pi^2 r_0^2 R_0) , \tag{A15}$$

we can obtain the result of Equation (14).

References

1. H. K. Liu and R. L. Kurtz, "A Practical Method for Holographic Interference Fringe Assessment," accepted for publication by J. of Opt. Engr., 1977. March/April 1977 Issue.

2. H. K. Liu, E. R. Commeens, W. D. Hunt, and L. Whitt, "Evaluation of a Composite Mobile Holographic Non-destructive Test System," BER Report No. 204-74, College of Engr. Univ. of Ala., Univ., Ala. 35486, 1976.

3. Espy, P. N., A Feasibility Study of the Nondestructive Evaluation of Solder Joints by Optical Correlation, unpublished Ph.D. dissertation, U. of Arkansas, 1974.

4. Jenkins, R. W. and McIlwain, M. C., "Solder Joint Fatigue Measurement by Optical Cross-Correlation," in Holography and Optical Filtering, NASA SP-299, 1973.

5. Vander Lugt, A., "Signal Detection by Complex Spatial Filtering," IEEE Trans. Inform. Th., 10, 139 (1964).

6. Papoulis, A., Systems and Transforms with Applications in Optics, McGraw-Hill, 1968.

7. Chuang, K. C., "Application of the Optical Correlation Measurement to Detection of Fatigue Damage," Materials Eval., 26, 116 (1968).

8. Marom, E., "Real-Time Strain Measurements by Optical Correlation," Appl. Opt., 9, 1385 (1970).

References (Continued)

9. P. Beckmann and A. Spizzichino, The Scattering of Electromagnetic Waves from Rough Surfaces (MacMillan, N. Y., 1963).

10. J. S. Bendat, Principles and Applications of Random Noise Theory (Wiley, N. Y., 1958).

11. Joachim C. Erdmann and Robert I. Gellert, J. Opt. Soc. Am., 66, 1194 (1976).

12. J. S. Bendat, Principles and Applications of Random Noise Theory (Wiley, New York, 1958), p. 129.

13. E. Madelung, Die Machematischem Hilfsmittel des. Physikers (Springer, Berlin, 1957), p. 80.

14. T. Hagfors, "Relations Between Rough Surfaces and Their Scattering Properties as Applied to Radar Astronomy," in Radar Astronomy, edited by J. V. Evans and T. Hagfors (McGraw-Hill, New York, 1968), p. 187.